arXiv:1607.03911v1 [cond-mat.soft] 13 Jul 2016

Thermal diode made by nematic liquid crystal

Djair Melo, Ivna Fernandes

Instituto de Física, Universidade Federal de Alagoas, Av. Lourival Melo Mota, s/n, 57072-900 Maceió, AL, Brazil

Fernando Moraes

Departamento de Física, CCEN, Universidade Federal da Paraíba, Caixa Postal 5008, 58051-900 , João Pessoa, PB, Brazil

Departamento de Física, Universidade Federal Rural de Pernambuco, 52171-900 Recife, PE, Brazil

Sébastien Fumeron

Institut Jean Lamour, Université de Lorraine, BP 239, Boulevard des Aiguillettes, 54506 Vandœuvre les Nancy, France

Erms Pereira[1]

Escola Politécnica de Pernambuco, Universidade de Pernambuco, Rua Benfíca, 455, Madalena, 50720-001 Recife, PE, Brazil

Abstract

This work investigates how a thermal diode can be designed from a nematic liquid crystal confined inside a cylindrical capillary. In the case of homeotropic anchoring, a defect structure called escaped radial disclination arises. The asymmetry of such structure causes thermal rectification rates up to 3.5% at room temperature, comparable to thermal diodes made from carbon nanotubes. Sensitivity of the system with respect the heat power supply, the geometry of the capillary tube and the molecular anchoring angle is also discussed.

Keywords: Classical Fourier-law analysis, Thermal diodes, Liquid crystal, Escaped radial disclination, Thermal rectification, Anchoring angle.

Email address: djfmelo@gmail.com (Djair Melo)

[1]On leave from: Instituto de Física, Universidade Federal de Alagoas, Av. Lourival Melo Mota, s/n, 57072-900 Maceió, AL, Brazil.

1. Introduction

Although the grounds of thermodynamics were formulated by Sadi Carnot as far back as 1824, controlling heat flows is still a challenging topic. Besides its academic interest, the worldwide raise of energy consumption made wasted heat collection and revalorization a major issue. As a consequence, studies dedicated to thermal management are now receiving considerable attention [1, 2]. Among these, there are studies on designing the thermal analogs of usual electronic components, such as thermal logic gates [3] or thermal transistors [4–6]. Controlled phonon transport has been obtained with from expensive nanostructured artificial devices that can perform concentrating, shielding or inverting of conductive heat flux [7–10]. Thermal rectification generally arises because of an asymmetry of the system along the direction of heat propagation and non-linear thermal properties [11–17], allowing some of these devices being understood by classical Fourier-law analysis [18–21]. This is usually achieved either by relying on asymmetric geometries such as constricted nanotubes [6], or by gradients of physical properties (e.g. pore density in a nanowire [13]).

A recent work emphasizes on the assets of nematic liquid crystals (NLC) for controlling heat flows [22]: contrary to nanostructured devices [10, 23, 24], the inner structure of NLC comes from weak stresses (electric, mechanical...) and/or anchoring conditions and therefore, the NLC-based device can be tuned at will for heat conduction. This is possible because NLC are made by anisotropic molecules that exhibits a stable phase between the crystalline solid and isotropic liquid phases with, therefore, intermediate properties: the nematic phase. In such phase, the molecules present orientational order, but not positional, and they are aligned on average along a specific direction represented by a unit vector field $\hat{n}\left(\vec{r}\right)$, known as the *director* field. In particular, the required asymmetry for the thermal rectification effect can easily be obtained from a NLC confined inside a capillary tube with homeotropic boundary conditions. Indeed, as studied by several authors [25–27], a funnel-shaped configuration of the director field (known as an escaped radial disclination) may occur (Fig. 1). The possibility of manipulation of escaped disclinations by use of laser tweezers [28] creates new possibilities for its use in optical or thermal devices like the one proposed here.

In this paper, we investigate the possibility to design thermal diodes from confined NLC in cylindrical cavities [26, 27, 29–37] endowed with an escaped radial disclination. Firstly, the thermal conductivity tensor is determined from algebraic properties of the director field $\hat{n}\left(\vec{r}\right)$, including the temperature dependence of the principal molecular thermal conductivities. Secondly, calculation of the rectification factor using the experimental data of 5CB [38] is performed with the following boundary conditions: a constant temperature is set at one base of the capillary tube,

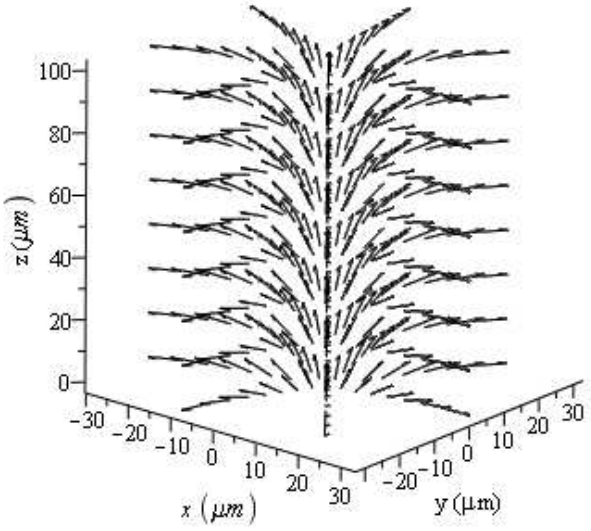

Figure 1: Rod-like molecules forming an escaped radial disclination with escape in $-\hat{z}$ direction in a capillary tube (not shown) with radius $R = 30\ \mu m$ and height $h = 100\ \mu m$.

whereas inward heat flows through the other base. The remainder is thermally insulated. Reversing that configuration shows a rectification effect. Finally, we study the influence of the heat power, the geometry and the anchoring angle on the efficiency of the presented thermal diode, obtaining rectifications up to 3.5%, that is higher than the rectification of thermal diodes made by carbon nanotubes and similar to the ones made by boron nitride nanotubes [13]. The same strategy here developed can be applied to different anisotropic materials that present similar orientation field in in a solid state.

2. Model and formalism

The proposed thermal diode consists of an escaped radial disclination with escape in the $-\hat{z}$ direction [26, 27, 37], Fig. 1. The spatial dependence of the director $\hat{n}\left(\vec{r}\right)$ in the capillary tube is obtained by solving the Euler-Lagrange equation, with the

suitable boundary conditions of this system, of the free elastic energy density [27]

$$\begin{aligned} f =& \frac{1}{2}(K_{11}\left(div\ \hat{n}\right)^2 + K_{22}\left(\hat{n}\cdot curl\ \hat{n}\right)^2 \\ &+ K_{33}\left(\hat{n}\times curl\ \hat{n}\right)^2), \end{aligned}$$

where K_{11}, K_{22} and K_{33} are respectively the curvature elastic constants of the distortions named *splay*, *twist* and *bend*. On the one-constant approximation ($K_{11} \approx K_{22} \approx K_{33} \equiv K$) and imposing homeotropic condition for the director $\hat{n}$ at the wall of the capillary tube, we study the rectification related to the strong and weak anchoring regimes using the algebraic expression of the spatial director field $\hat{n}\left(\vec{r}\right)$. From the possible representations of $\hat{n}\left(\vec{r}\right)$ found in [25, 26], we choose the one in [26] due to its simplicity, such that, for the strong and the weak anchoring regimes, they are respectively

$$\chi\left(r\right) = 2\arctan\left(\frac{r}{R}\right), \tag{1}$$

and

$$\chi\left(r\right) = 2\arctan\left(\frac{r}{R}\tan\left(\frac{\chi_0}{2}\right)\right), \tag{2}$$

where R is the radius of the capillary tube, $\chi\left(r\right)$ is the angle between the director and the axis of the capillary and $\chi_0 \equiv \chi\left(r=R\right)$ is the anchoring angle. The physical ideas on energy and their algebraic deduction used on the obtaining of the eqs. (1) and (2) for the escaped radial disclination are found in [26]. Observe that the algebraic manifestation of the weak anchoring regime is a pretilt with $\chi_0 < \frac{\pi}{2}$ [26].

With (1) and (2), one can write the director of the escaped radial disclination

$$\hat{n} = \left(\sin\chi\left(r\right),\ 0,\ \cos\chi\left(r\right)\right), \tag{3}$$

in cylindrical coordinates and apply it in the equation of the components of the thermal conductivity tensor [27],

$$\lambda^{ij} = \lambda_{iso}\delta^{ij} + \lambda_a\left(n^i n^j - \frac{\delta^{ij}}{3}\right), \tag{4}$$

where δ^{ij} are the elements of the homogeneous isotropic thermal conductivity tensor written in the cylindrical coordinates and

$$\begin{aligned} \lambda_{iso} &= \frac{\lambda_\parallel + 2\lambda_\perp}{3}, \\ \lambda_a &= \lambda_\parallel - \lambda_\perp, \end{aligned}$$

being $\lambda_{\parallel}$ and $\lambda_{\perp}$ respectively the molecular thermal conductivities parallel and perpendicular to the major molecular axis, where $\lambda_{\parallel} > \lambda_{\perp}$. This result with the spatial asymmetry produced by the escaped radial disclination allow us to expect that the direction of the "direct" thermal setup, the direction that produces the higher bulk thermal conductivity, is the one of the escape: $-\hat{z}$ direction. Therefore, our proposed thermal diode behaves in a similar way to ballistic thermal diodes [20, 21].

Thus the present model could be well developed considering the temperature independence of the principal thermal conductivities and this simplified scenario would generate a robustness on the thermal anisotropy of the escaped radial disclination against the used heat power. However, as the employed liquid crystal, 5CB, is a thermotropic NLC, the temperature changes the scalar order parameter and, consequently, their principal molecular thermal conductivities $\lambda_{\parallel}$ and $\lambda_{\perp}$. Considering the influence of the temperature on the scalar order parameter, such temperature dependences of the thermal conductivities are implemented using the following nonlinear equations and parameter data extracted from [38]:

$$\begin{aligned} \lambda_{\parallel} &= \lambda_0 + \lambda_1 \times (T - T_{NI}) + \lambda_{1,\parallel} (T_c - T)^{\alpha_{\parallel}} , \\ \lambda_{\perp} &= \lambda_0 + \lambda_1 \times (T - T_{NI}) + \lambda_{1,\perp} (T_c - T)^{\alpha_{\perp}} , \end{aligned} \tag{5}$$

where

$$\begin{aligned} \lambda_0 &= 1.512, \\ \lambda_1 &= 0.00370, \\ T_{NI} &= 308.32\ K, \\ \lambda_{1,\parallel} &= 0.4026, \\ \lambda_{1,\perp} &= -0.1448, \\ T_c &= 309.21\ K, \\ \alpha_{\parallel} &= 0.237, \\ \alpha_{\perp} &= 0.172. \end{aligned}$$

With the nonlinear behavior of (5), we expect this additional factor facilitates the thermal rectification, as reported by the literature [6, 8, 12, 14, 18–21, 39].

3. Results and discussion

3.1. Asymmetric thermal boundary conditions

We now implement, on the strong anchoring regime with the angle $\chi(r)$ between the director and the plane $x - y$ given by (1), an escaped radial disclination in the

$-\hat{z}$ direction inside a capillary tube with radius $R = 30\ \mu m$ and height $h = 100\ \mu m$ in a finite element simulation using COMSOL Multiphysics, Fig. 1. The whole tube is set at initial temperature of 296 K. One of the bases of the cylinder is set at 296 K, heat is pumped in at a rate of 5 $\frac{kW}{m^2}$ across the other one and thermal insulation is set at the lateral surface. These information are implemented in our simulation to solve, in steady-state regime and in the absence of internal sources, the Fourier and Laplace equations [40]

$$q^i = -\lambda^{ij}\partial_j T,$$
$$\nabla \cdot \vec{q} = \partial_i \left[\lambda^{ij}\partial_j T\right] = 0,$$

where q^i are the components of the heat flux $\vec{q}$ and T is the temperature field. The results are shown on Fig. 2.

To determine the rectification, we use the following definition:

$$Rectification = \frac{\Delta T_i - \Delta T_d}{\Delta T_d} \times 100 \quad \%, \tag{6}$$

where $\Delta T_i = T_{i,h} - 296$ is the difference between the high temperature produced by the heat pumped in the cylinder, $T_{i,h}$, when working in the inverse setup and the low temperature of 296 K (similarly, we have $\Delta T_d = T_{d,h} - 296$ when working in the direct setup).

From the simulations of the capillary tube, represented in the Fig. 2, we observed that the downward flux produces the lower difference on the temperatures, meaning that this direction has the higher thermal conductance, representing the direct setup of the thermal diode. With the values of ΔT_i and ΔT_d of this capillary tube, the eq. (6) produces a rectification effect of 1.5%, similar to the one produced by carbon nanotubes [13] at room temperature. This rectification can be explained considering the spatial asymmetry produced by the escape in $-\hat{z}$ direction, in a similar way to ballistic rectification [20, 21] due to spatial asymmetries, or considering the addition of an effective curvature felt by the phonons on such direction [22, 41], once $\lambda_{\parallel} > \lambda_{\perp}$, promoting a higher thermal conductivity in the direction of the escape.

3.1.1. Efficiency of the thermal diode

We analyzed the efficiency of the rectification due to the heat power supply, to the geometry of the capillary tube and to the molecular anchoring angle at the surface of the tube. The heat powers were chosen to produce temperatures bellow the nematic-isotropic transition temperature T_{NI} in eq. (5), while the radii of the capillary tube were chosen to be far bigger than a typical value of the core radius

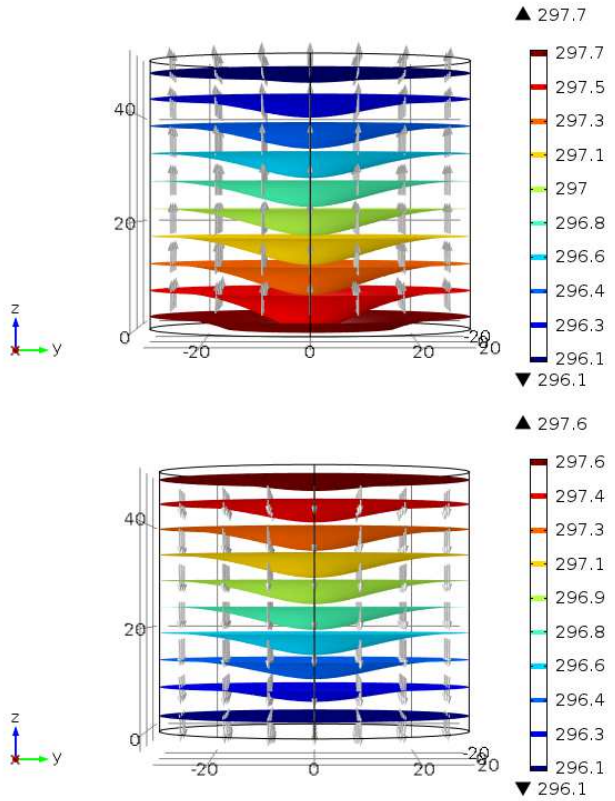

Figure 2: Isothermal surfaces of a liquid crystalline thermal diode in (up) inverse thermal setup and (bottom) direct thermal setup. The cylinder has radius 30 μm, height 50 μm, inward heat flux of 5 $\frac{kW}{m^2}$ at the base with high temperature and fixed temperature of 296 K at the other base. The rectification effect is 1.5%.

r_c of a radial disclination ($r_c \approx 500$ Å [27]), avoiding energy competition between the radial disclination and the escaped radial one [25]. The upper and lower limits for the height were assumed respecting experimental issues on the creation of the escaped radial disclination in the capillary tube (for example, the flow profile of the liquid crystal during the filling of the capillary tube [27] or the temperature rate during the cooling of the liquid crystal from the isotropic phase to the nematic one [26]).

Relative to the heat power and to the geometry of the capillary tube, the results are summarized in Fig. 3. It was observed that the rectification effect decreases with the heat power. Its reason is that more heat power implies in a higher temperature, decreasing the anisotropy $\lambda_{\parallel} - \lambda_{\perp}$, as can be seen by the equations (5), reducing the

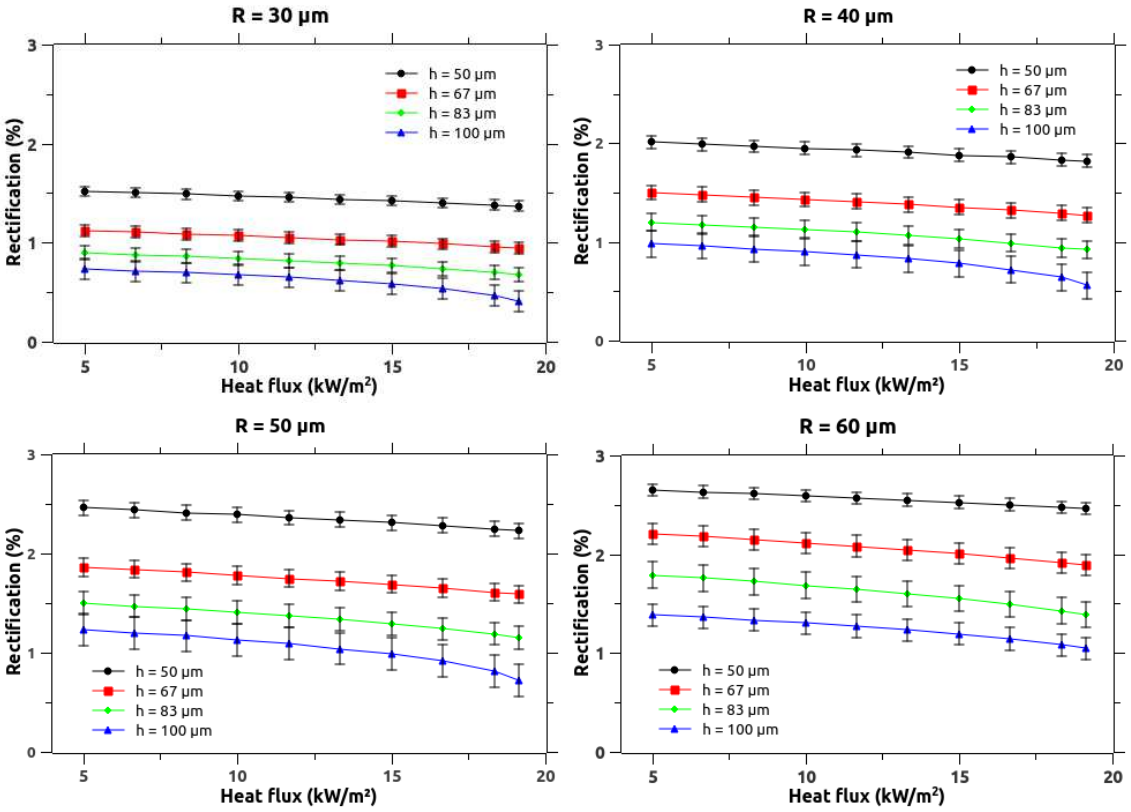

Figure 3: Rectification versus heat power produced by an escaped radial disclination in the strong anchoring regime, eq. (1), with different values of the radius R and the height h of its confining capillary tube.

rectification effect.

Relative to the geometry, it was observed in Fig. 3 that the rectification effect increases with increasing area of the bases and increases with decreasing height of the tube. About the influence of the area on the rectification, we justify the results noting that a large area denotes more heat flux to be deflected by the isothermal surfaces, enhancing the rectification. About the influence of the height on the rectification, the results suggest that when h/R is high, the device looks like a 1D wire, minimizing the effect of the escaped radial disclination on the heat flux, decreasing the rectification. Such dependence on the height favors the miniaturization of the diode, while the dependence on the area concurs to the application of this device on a large region, in opposite of its use on a small local.

Relative to the anchoring angle, we use eq. (2) in the simulations, where the

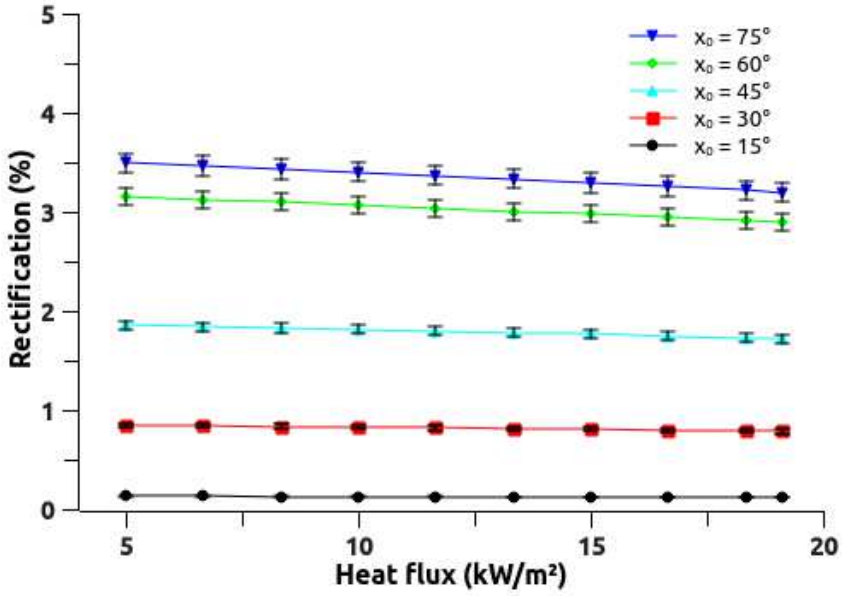

Figure 4: Rectification versus heat power produced by an escaped radial disclination in the weak anchoring regime, eq. (2), inside a capillary tube with radius $R = 60\ \mu m$, height $h = 50\ \mu m$, with different anchoring angles $\chi_0 < 90°$.

rectification for different values of the anchoring angle $\chi_0 < 90°$ are found in Fig. 4 with radius $R = 60\ \mu m$ and height $h = 50\ \mu m$, obtaining a rectification up to 3.5%, that is higher than the rectification obtained by carbon nanotubes and comparable to the ones made by boron nitride nanotubes [13]. Comparing this value with the results in Fig. 3, we notice an increased rectification with $\chi_0 = 75°$ and $\chi_0 = 60°$ and a monotonically decrease from $\chi_0 = 75°$ to $\chi_0 = 15°$. The behavior is explained by a reduction on the anisotropy of the capillary tube and, consequently, on the effective curvature felt by the phonons [42] and by the heat flux [41], once the spatial configuration of the director $\hat{n}$ approaches to the uniform $\hat{n} = \hat{z}$. This also implies the existence of an optimized anchoring angle χ_0 that generates the maximum rectification. In fact, when we reduce the anchoring angle χ_0, reducing the axial anisotropy, it is expected that there is an ideal anchoring angle χ_{ideal} that maximizes the rectification. Below this χ_{ideal}, we obtain molecular configurations that makes the rectification decreases. This behavior is shown in Fig. 5, where the ideal anchoring angle is $\chi_{ideal} = 73°$. For anchoring angles smaller than $\chi_{ideal} = 73°$, the anisotropy starts to be destroyed, causing the thermal diode becomes uniform throughout the capillary tube.

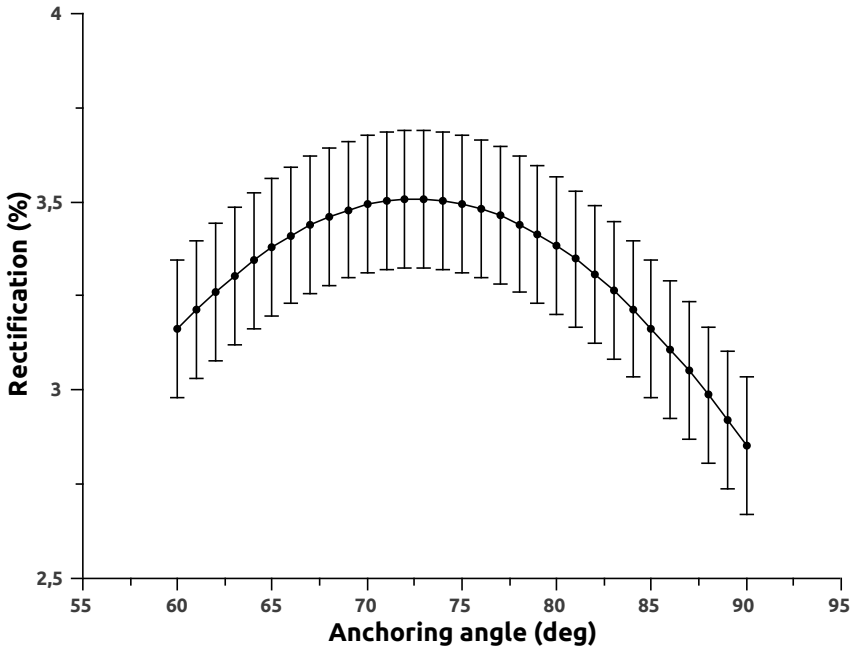

Figure 5: Rectification versus anchoring angles χ_0 produced by an escaped radial disclination in the weak anchoring regime inside a capillary tube with radius $R = 60\ \mu m$, height $h = 50\ \mu m$ and heat flux 5 $\frac{kW}{m^2}$.

For different geometries and anchoring regimes, our simulations resulted in temperatures near to $T_{NI} = 308.32\ K$ at heat fluxes from 19 $\frac{kW}{m^2}$, for radius 30 μm, height 100 μm and anchoring angle $\chi_0 = 0$, up to 37 $\frac{kW}{m^2}$, for radius 60 μm, height 50 μm and anchoring angle $\chi_0 = 15^{\circ}$. These results on heat flux, bigger than other reported one in [15], are explained due to their rectifications (using 5 $\frac{kW}{m^2}$, 0.73% for the first case and 3.5% for the latter one), because high rectifications presented low temperatures and, consequently, strong robustness for the heat flux. Thus eutectic mixtures could enlarge the heat power range and the temperature range, avoiding the loosing the desired anisotropy.

To isolate the asymmetric aspect from the nonlinear one of the rectification, we repeat the simulations disregarding the temperature dependence of $\lambda_{\parallel}$ and $\lambda_{\perp}$ and set them constant at 299.26 K [38]. The results are shown in Fig. 6. As can be seen, the constant molecular thermal conductivities produce rectifications that are proportional to the heat flux and that are low compared to Fig. 3. This shows that the nonlinear temperature dependences of the $\lambda_{\parallel}$ and $\lambda_{\perp}$ has strong influence on the rectification and the studied spatial anisotropy is enough for such phenomenon. The

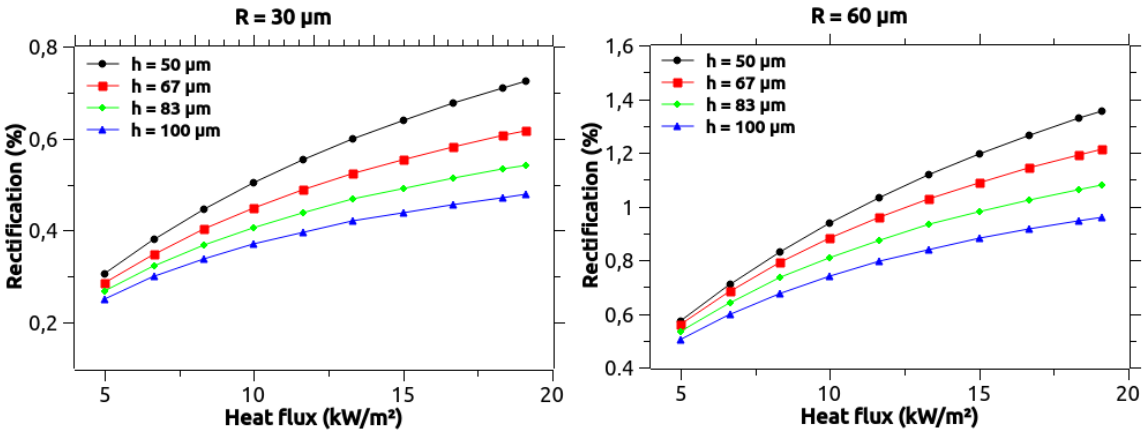

Figure 6: Rectification versus heat power produced by an escaped radial disclination with constant $\lambda_{\parallel}$ and $\lambda_{\perp}$ in the strong anchoring regime, eq. (1), with different values of the radius R and the height h of its confining capillary tube. The errors on the rectification range from 10^{-4} to 10^{-7}.

presence of the rectification due to the asymmetry can be understood by the tendency of the phonon to follow the director [41, 42], once $\lambda_{\parallel} > \lambda_{\perp}$, while the proportionality to the heat flux can be explained by the available heat to be deflected by isothermal surfaces, similar to the influence of the radius R.

3.2. Symmetric thermal boundary conditions

Using again eq. (5) and for symmetric thermal boundary conditions, where on both basis are set constant temperatures producing a temperature difference $\Delta T \equiv T_{high} - 296$ with $T_{high} \in [296\ K,\ 308\ K]$, we found the rectifications shown in Fig. 7, where it was used another definition for it [20]:

$$Rectification = \frac{Q_d - Q_i}{Q_i} \times 100 \quad \%, \tag{7}$$

where Q_d and Q_i $(Q_d > Q_i)$ are the heat flux in the direct (with $T(x = h) = T_{high}$ and $T(x = 0) = 296\ K$) and inverse (with $T(x = 0) = T_{high}$ and $T(x = h) = 296\ K$) setups respectively. From Fig. 7 we notice that the rectifications are proportional to the temperature bias set on the basis (unless of the last points for $R = 30\ \mu m$ and $h = 83\ \mu m$ and $h = 100\ \mu m$), consistent to [18–20], and are very low compared to the results from the asymmetric boundary conditions. This suggests our thermal diode based on liquid crystal works better as a heat flux thermal diode, when one sets a heat flux at one the basis, than a temperature bias thermal diode, when one sets constant

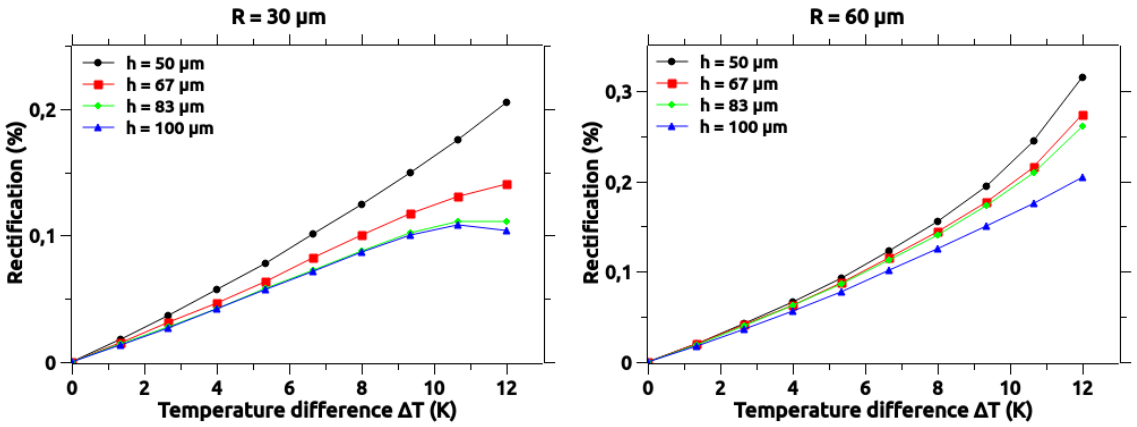

Figure 7: Rectification versus temperature difference$\Delta T \equiv T_{high} - 296$, with $T_{high} \in [296\ K,\ 308\ K]$, produced by an escaped radial disclination in the strong anchoring regime, eq. (1), with different values of the radius R and the height h of its confining capillary tube. The errors on the rectification range from 10^{-4} to 10^{-7}.

temperatures on the basis. As shown in [18], Neumann theorem forbids asymmetrical transport if the inner structure is symmetrical and if the thermal conductivity is temperature independent. The fact that we have neither, allows us to have a greater asymmetry in the heat flux when the boundary conditions change form temperature bias to heat injection. We can also think of this in terms of phonon beams: depending on the way they traverse the device, they are either focused or defocused due to the asymmetic director field configuration. This effect has been observed experimentally for light beams in escaped disclinations, as reported in [43]. This can indicate that the phonons that start to move from the fixed higher temperature to the fixed lower one fell less spatial anisotropy of the thermal conductivity than the phonons that already are in motion due to the external heat flux set on one of the terminals of the diode. We also notice in Fig. 7 for $R = 30\ \mu m$ a decreasing on the rectification for $\Delta T = T_{high} - 296 \approx 12\ K \Rightarrow T_{high} \approx 308\ K$. This can be understood as a competition between the available heat flux due the ΔT and the annihilation of the anisotropy between the molecular thermal conductivities $\lambda_{\parallel}$ and $\lambda_{\perp}$near to the nematic-isotropic phase transition T_{NI}.

4. Summary and conclusions

The present paper continues recent studies [22, 41] that explore the possibilities offered by NLC for heat transfer management and their technological applications for phononics. We proposed a thermal diode made of nematic liquid crystal, that

consists in an escaped radial disclination of the liquid crystal 5CB in a capillary tube. Once the parallel molecular thermal conductivity of the NLC is higher than the perpendicular one, the direction that the thermal diode conducts (the direct thermal setup) is on the escape of the disclination. For different values of the radius and height of the tube and the anchoring angles at the capillary walls, rectification effects are observed in our simulations up to 3.5% at room temperature. Increasing heat power and the height of the tube decrease the rectification effect, while increasing the area of the tube increases this phenomenon. Such dependence on the geometry would lead to miniaturization of the device and its application on a vast surface. We found that our thermal diode works better as a heat flux thermal diode, pumping heat in the diode, than a temperature bias thermal diode, setting a fixed difference temperature on the terminals of the diode. We also noticed that the spatial anisotropy alone of the thermal conductivity produces the thermal rectification for our proposed thermal diode, with low rectifications when compared with the ones produces by the spatial asymmetry plus temperature non-linearities.

The results presented in this article were based on four factors: a physically anisotropic molecular arrangement, temperature dependence of the thermal conductivities, the existence of a nematic phase and the possibility of elastic deformations (topological defects) in the nematic phase. Thus, our results apply to lyotropic liquid crystals, once they have three of these factors [44, 45], and any other materials that sustains such director configurations in a nematic phase, as ferronematics [46–48]. With the prospect of having glassy liquid crystals [49, 50], it is possible to release the escaped radial disclination from its capillary tube, enlarging the technological applications of the presented thermal diode.

A natural extension of this work is to design thermal transistors [4–6] from liquid crystals. The idea is to explore the non-linearity of the principal thermal conductivities in Fourier's equation to find thermally stable states that "cut" and "release"' the heat flow or that amplify it.

Acknowledgements

F.M. and E.P. acknowledges CAPES, CNPq, and E.P. to FAPEAL (Brazilian agencies) for the financial support. The authors thank the anonymous referees for the comments.

References

[1] M. Biercuk, M. C. Llaguno, M. Radosavljevic, J. Hyun, A. T. Johnson, J. E. Fischer, Carbon nanotube composites for thermal management, Applied physics

letters 80 (15) (2002) 2767–2769.

[2] H. Huang, C. Liu, Y. Wu, S. Fan, Aligned carbon nanotube composite films for thermal management, Advanced materials 17 (13) (2005) 1652–1656.

[3] L. Wang, B. Li, Thermal logic gates: Computation with phonons, Phys. Rev. Lett. 99 (2007) 177208.

[4] B. Li, L. Wang, G. Casati, Negative differential thermal resistance and thermal transistor, Appl. Phys. Lett. 88 (2006) 143501.

[5] O. P. Saira, M. Meschke, F. Giazotto, A. M. Savin, M. Mottonen, J. P. Pekola, Heat transistor: Demonstration of gate-controlled electronic refrigeration, Phys. Rev. Lett. 99 (2007) 027203.

[6] N. Li, J. Ren, L. Wang, G. Zhang, P. Hanggi, B. Li, Colloquium: Phononics: Manipulating heat flow with electronic analogs and beyond, Rev. Mod. Phys. 84 (2012) 1045.

[7] M. Maldovan, Narrow-low frequency spectrum and heat management by thermocrystals, Phys. Rev. Lett. 110 (2013) 025902:1–5.

[8] M. Maldovan, Sound and heat revolutions in phononics, Nature 503 (2013) 209.

[9] S. Narayana, Y. Sato, Heat flux manipulation with engineered thermal materials, Phys. Rev. Lett. 108 (2012) 214303:1–5.

[10] S. Guenneau, C. Amra, D. Veynante, Transformation thermodynamics: cloaking and concentrating heat flux, Opt. Exp. 20 (2012) 8207.

[11] M. Terrano, M. Peyrard, G. Casati, Controlling the energy flow in nonlinear lattices: A model for a thermal rectifier, Phys. Rev. Lett. 88 (2002) 094302.

[12] B. Li, L. Wang, G. Casati, Thermal diode: Rectification of heat flux, Phys. Rev. Lett. 93 (2004) 184301.

[13] C. W. Chang, D. Okawa, A. Majumdar, A. Zettl, Solid-state thermal rectifier, Science 314 (2006) 1121.

[14] Z. Chen, C. Wong, S. Lubner, S. Yee, J. Miller, W. Jang, C. Hardin, A. Fong, J. E. Garay, C. Dames, A photon thermal diode, Nature Communications 5 (2014) 5446.

[15] H. Tian, D. Xie, Y. Yang, T.-L. Ren, G. Zhang, Y.-F. Wang, C.-J. Zhou, P.-G. Peng, L.-G. Wang, L.-T. Liu, A novel solid-state thermal rectifier based on reduced graphene oxide, Scientific reports 2.

[16] M. Schmotz, J. Maier, E. Scheer, P. Leiderer, A thermal diode using phonon rectification, New Journal of Physics 13 (11) (2011) 113027.

[17] D. Sawaki, W. Kobayashi, Y. Moritomo, I. Terasaki, Thermal rectification in bulk materials with asymmetric shape, Applied Physics Letters 98 (8). doi:http://dx.doi.org/10.1063/1.3559615.
URL http://scitation.aip.org/content/aip/journal/apl/98/8/10.1063/1.3559615

[18] H. Hoff, Asymmetrical heat conduction in inhomogeneous materials, Physica A: Statistical Mechanics and its Applications 131 (2) (1985) 449–464.

[19] B. Hu, D. He, L. Yang, Y. Zhang, Thermal rectifying effect in macroscopic size, Physical Review E 74 (6) (2006) 060201.

[20] C. Dames, Solid-state thermal rectification with existing bulk materials, Journal of Heat Transfer 131 (6) (2009) 061301.

[21] J. Miller, W. Jang, C. Dames, Thermal rectification by ballistic phonons in asymmetric nanostructures, in: ASME 2009 Heat Transfer Summer Conference collocated with the InterPACK09 and 3rd Energy Sustainability Conferences, American Society of Mechanical Engineers, 2009, pp. 317–326.

[22] S. Fumeron, E. Pereira, F. Moraes, Principles of thermal design with nematic liquid crystals, Phys. Rev. E 89 (2014) 020501. doi:10.1103/PhysRevE.89.020501.
URL http://link.aps.org/doi/10.1103/PhysRevE.89.020501

[23] T. Han, T. Yuan, B. Li, C.-W. Qiu, Homogeneous thermal cloak with constant conductivity and tunable heat localization, Sci. Rep. 3 (2013) 1593.

[24] T. Han, X. Bai, J. T. Thong, B. Li, C.-W. Qiu, Full control and manipulation of heat signatures: Cloaking, camouflage and thermal metamaterials, Advanced Materials 26 (11) (2014) 1731–1734.

[25] P. Cladis, M. Kleman, Non-singular disclinations of strength s = + 1 in nematics, J. Physique 33 (1972) 591.

[26] G. Crawford, D. W. Allender, J. Doane, Surface elastic and molecular-anchoring properties of nematic liquid crystals confined to cylindrical cavities, Physical Review A 45 (12) (1992) 8693.

[27] P. Oswald, P. Pieranski, Nematic and cholesteric liquid crystals: concepts and physical properties illustrated by experiments, CRC press, 2005.

[28] I. I. Smalyukh, B. I. Senyuk, S. V. Shiyanovskii, O. D. Lavrentovich, A. N. Kuzmin, A. V. Kachynski, P. N. Prasad, Optical trapping, manipulation, and 3d imaging of disclinations in liquid crystals and measureme Molecular Crystals and Liquid Crystals 450 (1) (2006) 79/[279]–95/[295]. arXiv:http://dx.doi.org/10.1080/15421400600587787, doi:10.1080/15421400600587787.
URL http://dx.doi.org/10.1080/15421400600587787

[29] C. E. Williams, P. E. Cladis, M. Kleman, Screw disclinations in nematic samples with cylindrical symmetry, Molecular Crystals and Liquid Crystals 21 (3) (1973) 355. arXiv:http://dx.doi.org/10.1080/15421407308083329, doi:10.1080/15421407308083329.
URL http://dx.doi.org/10.1080/15421407308083329

[30] S. Burylov, Equilibrium configuration of a nematic liquid crystal confined to a cylindrical cavity, Sov Phys JETP 85 (5) (1997) 873–886.

[31] M. Kuzma, M. M. Labes, Liquid crystals in cylindrical pores: Effects on transition temperatures and singularities, Molecular Crystals and Liquid Crystals 100 (1983) 103.

[32] I. Vilfan, M. Vilfan, S. Žumer, Defect structures of nematic liquid crystals in cylindrical cavities, Phys. Rev. A 43 (1991) 6875–6880. doi:10.1103/PhysRevA.43.6875.
URL http://link.aps.org/doi/10.1103/PhysRevA.43.6875

[33] G. P. Crawford, M. Vilfan, J. W. Doane, I. Vilfan, Escaped-radial nematic configuration in submicrometer-size cylindrical cavities: Deuterium nucle Phys. Rev. A 43 (1991) 835–842. doi:10.1103/PhysRevA.43.835.
URL http://link.aps.org/doi/10.1103/PhysRevA.43.835

[34] D. Zografopoulos, E. E. Kriezis, T. Tsiboukis, Photonic crystal-liquid crystal fibers for single-polarization or high-birefringence guidance, Optics express 14 (2) (2006) 914–925.

[35] X. Wang, M. Xu, H. Ren, Q. Wang, A polarization converter array using a twisted-azimuthal liquid crystal in cylindrical polymer cavities, Optics express 21 (13) (2013) 16222–16230.

[36] J. Jeong, L. Kang, Z. S. Davidson, P. J. Collings, T. C. Lubensky, A. Yodh, Chiral structures from achiral liquid crystals in cylindrical capillaries, Proceedings of the National Academy of Sciences 112 (15) (2015) E1837–E1844.

[37] R. D. Polak, G. P. Crawford, B. C. Kostival, J. W. Doane, S. Zumer, Optical determination of the saddle-splay elastic constant k24 in nematic liquid crystals, Phys. Rev. E 49 (1994) R978.

[38] G. Ahlers, D. S. Cannell, L. I. Berge, S. Sakurai, Thermal conductivity of the nematic liquid crystal 4- n -pentyl-4'-cyanobiphenyl, Phys. Rev. E 49 (1994) 545–553. doi:10.1103/PhysRevE.49.545.
URL http://link.aps.org/doi/10.1103/PhysRevE.49.545

[39] L. Wang, B. Li, Phononics gets hot, Physics World (2008) 27–29.

[40] M. N. Ozisik, Heat Conduction, 2nd Edition, John Wiley and Sons, New York, 1993.

[41] S. Fumeron, E. Pereira, F. Moraes, Modeling heat conduction in the presence of a dislocation, Int. J. Therm. Sci. 67 (2013) 64–71.

[42] E. Pereira, S. Fumeron, F. Moraes, Metric approach for sound propagation in nematic liquid crystals, Physical Review E 87 (2) (2013) 022506.

[43] Nematic topological line defects as optical waveguides, Vol. 9384. doi:10.1117/12.2079096.
URL http://dx.doi.org/10.1117/12.2079096

[44] F. L. S. Cuppo, A. M. Figueiredo Neto, S. L. Gómez, P. Palffy-Muhoray, Thermal-lens model compared with the sheik-bahae formalism in interpreting z-scan experiments on lyotropic liquid crystals, JOSA B 19 (6) (2002) 1342–1348.

[45] D. T. McCormick, K. D. Stovall, C. A. Guymon, Photopolymerization in pluronic lyotropic liquid crystals: Induced mesophase thermal stability, Macromolecules 36 (17) (2003) 6549–6558.

[46] C. Matuo, F. Tourinho, M. Souza, J. Depeyrot, A. Figueiredo Neto, Lyotropic ferronematic liquid crystals based on new ni, cu and zn ionic magnetic fluids, Brazilian journal of physics 32 (2B) (2002) 458–463.

[47] C. Sátiro, Light paths in a ferronematic cell, Physical Review E 80 (4) (2009) 042701.

[48] V. Zadorozhnii, A. Vasilev, V. Y. Reshetnyak, K. Thomas, T. Sluckin, Nematic director response in ferronematic cells, EPL (Europhysics Letters) 73 (3) (2006) 408.

[49] C. Van Oosten, K. Harris, C. Bastiaansen, D. Broer, Glassy photomechanical liquid-crystal network actuators for microscale devices, The European Physical Journal E 23 (3) (2007) 329–336.

[50] G.-Y. Yeap, T.-C. Hng, W. A. K. Mahmood, E. Gorecka, D. Takeuchi, K. Osakada, Novel nonsymmetric trimeric liquid crystals exhibiting glassy nematic state at low temperatures, Molecular Crystals and Liquid Crystals 487 (1) (2008) 135–152.